Front. Phys.
DOI 10.1007/s11467-011-0183-2

RESEARCH ARTICLE

Local density of states around two nonmagnetic impurities in cuprate superconductors

Zhan-peng HUANG, Xia-xia WAN, Feng YUAN†

College of Physics Science, Qingdao University, Qingdao 266071, China

E-mail: †qdyuanfeng@gmail.com

Received March 2, 2011; accepted March 15, 2011

The local density of states (LDOS) around two nonmagnetic impurities which are located at different sites is studied within the two-dimensional t–J–U model. The order parameters are determined in a self-consistent way with the Gutzwiller projected mean-field approximation and the Bogoliubov–de Gennes theory. When the two impurities are located one or two sites away, we find the superconductivity coherence peaks are more strongly suppressed and the zero-energy peak (ZEP) has split into two peaks. Whereas when the two impurities are located next to each other, the ZEP vanished, and LDOS does not change a lot compared with the case away from the impurities.

Keywords local density of states (LDOS), nonmagnetic impurities, Gutzwiller approximation

PACS numbers 74.62.Dh, 74.72.Ek, 76.75.+i

1 Introduction

During the past two decades, the nonmagnetic impurities effect on the cuprates had attracted a lot of theoretical [1–13] and experimental [14–17] attention. A series of scanning tunneling microscopy (STM) experiments had provided detailed information on the local density of states (LDOS) around a single nonmagnetic impurity in $Bi_2Sr_2CaCu_2O_{8+\delta}$. Also, the theoretical work about the LDOS around the nonmagnetic impurity had involved much attention [6–10]. Zhu *et al.* [9, 10] indicated that around the nonmagnetic impurities the LDOS shows superconductivity peaks strongly suppressed and there is an zero-energy peak (ZEP) involved; while away from the nonmagnetic impurity, the LDOS shows a typical "V" shape.

However, how about two or more nonmagnetic impurities? Morr *et al.* [18, 20] studied the quantum interference between nonmagnetic impurities in d-wave superconductors. Motivated by their work, in his paper we investigated the LDOS around two nonmagnetic impurities in gossamer superconductors. During these work, how to deal with the strong relation effects showed in CuO_2 plane is the key to understand the unusual properties of these superconductors. Recently, Gutzwiller approximation was proved to be a useful tool in dealing with the strongly correlated systems [21–24]. We rightly account for the effects of the Gutzwiller projection of t–J–U hamiltonian by solving the Bogoliubov–de Gennes (BdG) equations, and figure out LDOS around two nonmagnetic impurities. The structure shows that when the two impurities are located next to each other, the LDOS around them are like that away from them; while when the two impurities located two sites away, the LDOS shows the case of single impurity, but the superconductivity peaks are more strongly suppressed than the single case due to the quantum interference of the two nonmagnetic impurities.

2 The model and formulation

We start from the t–J–U model on a square lattice:

$$H = -t\sum_{\langle i,j\rangle\sigma} C^{\dagger}_{i\sigma}C_{j\sigma} + J\sum_{\langle i,j\rangle} S_i\cdot S_j + U\sum_i n_{i\uparrow}\cdot n_{i\downarrow} + \sum_{i\sigma} U_i n_{i\sigma} - \mu\sum_{i\sigma} C^{\dagger}_{i\sigma}C_{i\sigma} \quad (1)$$

where $\langle i,j\rangle$ respects the sum of the nearest sites, $C^{\dagger}_{i\sigma}(C_{i\sigma})$ is the electron creation (annihilation) operator. $n_{i\sigma} = C^{\dagger}_{i\sigma}C_{i\sigma}$ is the electron number operator at i site. The spin operator reads $S_i = \frac{1}{2}\sum_{\sigma\sigma'} C^{\dagger}_{i\sigma}\overrightarrow{\sigma}_{\sigma\sigma'}C_{i\sigma}$, where $\overrightarrow{\sigma} = (\sigma_x, \sigma_y, \sigma_z)$ is the Pauli matrices. U is the on site Coulomb potential. μ stands for the chemical potential. $U_i = U_0\delta_{iI}$ is the scattering potential of the im-

purity site. To study the situation of two nonmagnetic impurities here, we will put the impurities on different sites respectively.

To study the above Hamiltonian with the Gutzwiller variational approach, we take the trial wave function $|\psi\rangle$ as

$$|\psi\rangle = P_{\rm G}|\psi_0(\Delta_d, \Delta_{af}, \mu)\rangle \tag{2}$$

where $P_{\rm G}$ is the Gutzwiller projection operator and it is defined as

$$P_{\rm G} = \Pi_i[1-(1-g)\hat{n}_{i\uparrow}\hat{n}_{i\downarrow}] \tag{3}$$

here g is a variational parameter which takes the value between 0 and 1. As detailed in Ref. [8], with the help of the trial wave function and the Gutzwiler approximation, we can get the following Gutzwiller renormalized hamiltonian:

$$H_{\rm eff} = -\sum_{\langle i,j\rangle\sigma} t_{\rm eff} C^{\dagger}_{i\sigma} C_{j\sigma} + \sum_{\langle i,j\rangle} J_{\rm eff} S_i \cdot S_j + U_d + \sum_{i\sigma} U_i n_{i\sigma} - \mu \sum_{i\sigma} C^{\dagger}_{i\sigma} C_{i\sigma} \tag{4}$$

where $t_{\rm eff} = g_t t$ and $J_{\rm eff} = g_s J$. $g_t(g_s)$ is the Gutzwiller renormalization factor which we can get from the Gutzwiller approximation,

$$g_t^{ij(\uparrow\uparrow)} = \frac{[\sqrt{(n_\uparrow - d)\delta} + \sqrt{d(n_\downarrow - d)}]_j [\sqrt{(n_\uparrow - d)\delta} + \sqrt{d(n_\downarrow - d)}]_i}{[\sqrt{n_\uparrow(1-n_\uparrow)}]_j [\sqrt{n_\uparrow(1-n_\uparrow)}]_i} \tag{5}$$

$$g_t^{ij(\downarrow\downarrow)} = \frac{[\sqrt{(n_\downarrow - d)\delta} + \sqrt{d(n_\uparrow - d)}]_j [\sqrt{(n_\downarrow - d)\delta} + \sqrt{d(n_\uparrow - d)}]_i}{[\sqrt{n_\downarrow(1-n_\downarrow)}]_j [\sqrt{n_\downarrow(1-n_\downarrow)}]_i} \tag{6}$$

$$g_s = \frac{\sqrt{[(n_\uparrow - n)(n_\downarrow - n)]_i}\sqrt{[(n_\uparrow - n)(n_\downarrow - n)]_i}}{\sqrt{[n_\uparrow(1-n_\downarrow)n_\downarrow(1-n_\uparrow)]_i}\sqrt{[n_\uparrow(1-n_\downarrow)n_\downarrow(1-n_\uparrow)]_j}} \tag{7}$$

Here $n_\uparrow(n_\downarrow)$ is the average spin-up (spin-down) electron number per site. d is the double occupation electron number per site.

Using the mean-field approximation, we obtain the following BdG equations:

$$\sum \begin{pmatrix} H_{ij} & F_{ij} \\ F^*_{ij} & -H^*_{ij} \end{pmatrix} \begin{pmatrix} u^n_j \\ v^n_j \end{pmatrix} = E_n \begin{pmatrix} u^n_j \\ v^n_j \end{pmatrix} \tag{8}$$

where

$$\begin{aligned} H_{ij} &= -\sum_\eta (g_t t + \frac{3}{4} g_s J \chi_{ij})\delta_{j,i+\eta} + (U_i - \mu)\delta_{ij} \\ F_{ij} &= -\sum_\eta \frac{3}{8} g_s J \Delta_{ij} \delta_{j,i+\eta} \end{aligned} \tag{9}$$

In the above equations, we have introduced the electron pairing order parameter and the uniform bond order respectively,

$$\Delta_\eta = \langle C_{i\downarrow} C_{i+\eta\uparrow} - C_{i\uparrow} C_{i+\eta\downarrow}\rangle_0 = \Delta(-\Delta), \text{ when } \eta = x(y) \tag{10}$$

$$\chi_{ij} = \chi = \langle C^{\dagger}_{i\uparrow} C_{i+\eta\uparrow} + C^{\dagger}_{i\downarrow} C_{i+\eta\downarrow}\rangle_0 \tag{11}$$

The order parameters Δ, χ and n can be determined self-consistently:

$$\Delta_{ij} = -\frac{1}{2}\left[\sum_{n=1}^{2N} (v^{n*}_j u^n_i + v^{n*}_i u^n_j) \tanh\left(\frac{1}{2}\beta E_n\right)\right] \tag{12}$$

$$\chi_{ij} = \sum_{n=1}^{2N} u^n_i u^{n*}_i f(E_n) + \sum_{n=1}^{2N} v^n_i v^{n*}_i [1 - f(E_n)] \tag{13}$$

$$n_i = \sum_{n=1}^{2N} |u^n_i|^2 f(E_n) + \sum_{n=1}^{2N} |v^n_i|^2 [1 - f(E_n)] \tag{14}$$

and

$$0 = \sum_{i,n} \left(\frac{\partial E_{i,n}}{\partial d_i}\right) \tag{15}$$

where $f(E) = 1/(\mathrm{e}^{\beta E} + 1)$ is Fermi–Dirac distribution function. In this paper, we focus on the effect of the multiple impurities, so we here take the pairing interaction $g = 1$.

3 Results and discussion

In the numerical calculation, we construct a superlattice with the square lattice $N_x \times N_y$ as a unit supercell which the impurities are located at different sites. Throughout this paper, we take the size of the unit supercell $N = 25 \times 25$, the number of supercell $N_c = 10 \times 10$. Then we can solve numerically the BdG equation and carry out an iteration until the self-consistent equations are satisfied. Hereafter, we set $t = 1$, and take $J/t = 0.3$, the temperature $T = 0.0001t$. The impurity potential is taken $U = 100t$, the chemical potential $\mu = -0.35t$.

First, we put the two nonmagnetic impurities at the sites (13, 13) (14, 13) and (13, 13) (15, 13) respectively. In Fig. 1, we show the spatial variation of the electron pairing order parameter Δ_d which defined as

$$\Delta_d(i) = \frac{1}{4}[\Delta_x(i) + \Delta_{-x}(i) - \Delta_y(i) - \Delta_{-y}(i)] \tag{1}$$

From Fig. 1, we can see that because of the presence of the nonmagnetic impurities, the electron pairing order parameter Δ_d is strongly suppressed at the impurities sites, especially in Fig. 1(b). We can see that even at the

site $(14, 13)$ the electron pairing order parameter Δ_d is also strongly suppressed.

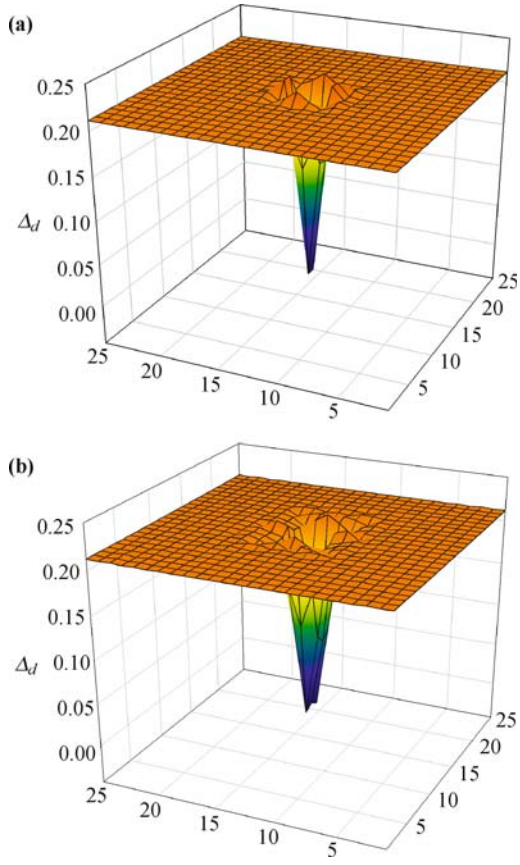

Fig. 1 The electron pairing order parameter of the two impurities localized at $(13, 13)\,(14, 13)$ **(a)** and at $(13, 13)\,(15, 13)$ **(b)**.

With the help of the obtained order parameters, we can further calculate the local density of states as

$$\rho_{\boldsymbol{i}}(E)_{\mathrm{T}} = -\frac{2}{M_x M_y}\sum_{n,\boldsymbol{k}}\left[\left|\boldsymbol{u}_{\boldsymbol{i}}^{n,\boldsymbol{k}}\right|^2 f'(E_{n,\boldsymbol{k}} - E) + \left|\boldsymbol{v}_{\boldsymbol{i}}^{n,\boldsymbol{k}}\right|^2 f'(E_{n,\boldsymbol{k}} + E)\right] \quad (2)$$

where the prefactor 2 comes from the spin sum, and $f'(E) = \mathrm{d}f(E)/\mathrm{d}E$ is the derivate of the fermi distribution function $f(E) = [\exp(\beta E) + 1]^{-1}$. The summation in $\rho_{\boldsymbol{i}}(E)_{\mathrm{T}}$ is averaged over $M_x \times M_y$ wavevectors in first Brillouin Zone. The LDOS $\rho_{\boldsymbol{i}}(E)$ is propotional to the local differential tunneling conductance which can be measured in a scanning tunneling microscope/spectroscopy experiment, so we can compare with our calculated LDOS with the STM results directly.

In Fig. 2, we plot the LDOS when the two nonmagnetic impurities localized at the site $(13, 13)\,(14, 13)$. From Fig. 2, we can see that for the site $(25, 13)$ which locates away from the impurities, LDOS shows a typical "V" shape, by exhibiting a gaplike feature with the gap edges at $\pm\Delta_{\max}$. Whereas, when the measure point is at site $(15, 13)$ which is near the two impurities, LDOS does not change a lot and the superconductor coherence peaks are suppressed only a little, and the energy gap also turns smaller. The same case is the site $(13, 12)$ that is also next to the impurities, which is very different from the case of single nonmagnetic impurity [8]. It appears that the two impurities do not affect the superconductor much.

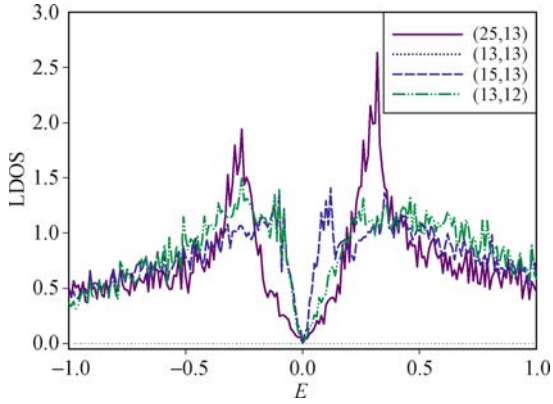

Fig. 2 Local density of state measured at different sites around (*dashed lines*) and far away (*solid line*) from the two impurities localized at $(13, 13)\,(14, 13)$.

However, in Fig. 3, our results of LDOS on the site $(14, 13)$ show that the effect of the two impurities is very large and obvious: the superconductor coherence peaks are strongly suppressed, and there is a very strong ZEP involved near the Fermi-energy. When the measure point is the site $(13, 12)$ the superconductor coherence peaks are also suppressed, and there is also a strong ZEP involved. The ZEP vanished at the site $(14, 12)$, which localized right under the $(14, 13)$ site. The case of $(25, 13)$ is the same with Fig. 2. It seems that the different distribution of the impurities has little effect on the sites which are far away from them.

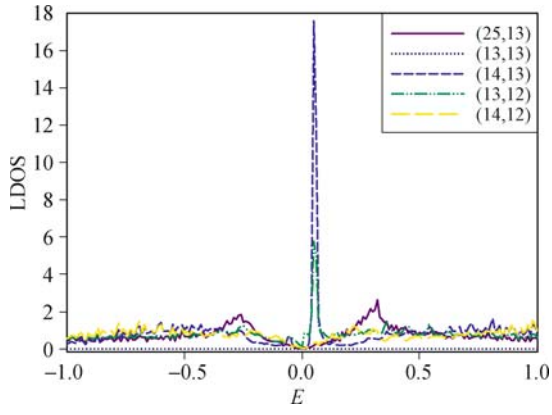

Fig. 3 Local density of state measured at different sites around (*dashed lines*) and far away (*solid line*) from the two impurities localized at $(13, 13)\,(15, 13)$.

Figure 4 displays the situation that the two nonmagnetic impurities located at sites $(13, 13)$ and $(17, 13)$ respectively. Figure 4(a) shows the LDOS around the impurity located at $(13, 13)$. We calculated the LDOS of the sites along the bond direction respectively. For the site $(14, 13)$ which is the nearest-neighbor site of the

impurity, we find that the superconducting coherence peaks are strongly suppressed, at the same time, near the Fermi-energy, there exists a strong ZEP. For the site (15, 13) which is the 3rd-neighbor site of the impurity, we can find that the ZEP cannot be seen. It indicate that the effect of the impurity is localized. All the results are like the situation of single nonmagnetic impurity. Figure 4(b) shows the LDOS around the impurity located at (14, 13). We calculated the LDOS of the sites along the nodal direction respectively. From Fig. 4(b) and compared with Fig. 4(a), we can find that LDOS of the sites along the bond direction is more strongly affected by the nonmagnetic impurities than that of the corresponding sites along the nodal direction. In other words, the intensity of the LDOS decays much faster along the gap nodal direction than along the bond direction. Our results are consistent with the experimental [14, 15] and previous theoretical results [1, 2].

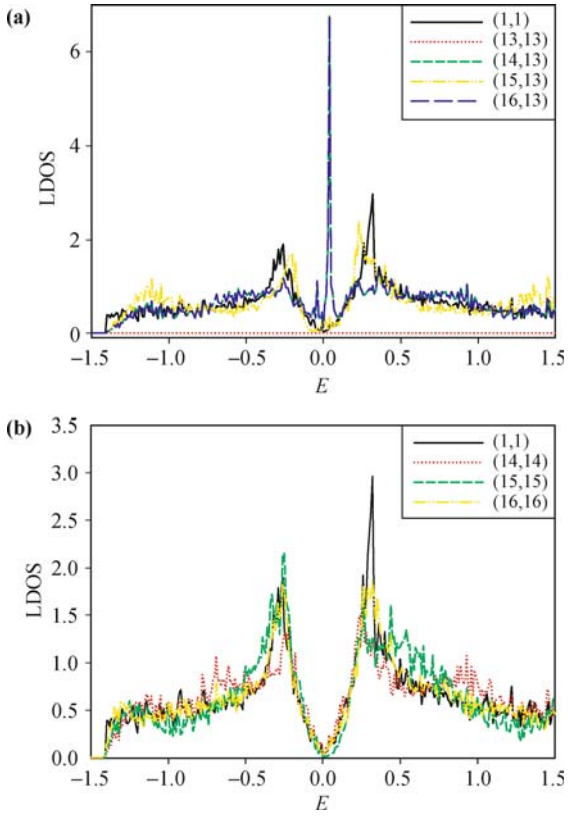

Fig. 4 Local density of state measured at different sites around (*dashed lines*) and far away (*solid line*) from the two impurities localized at (13, 13) (17, 13).

4 Summary

In conclusion, we studied the LDOS around and away from two nonmagnetic impurities which are located at different sites using Gutzwiller approximation in t–J–U model. We found that when the two impurities are located next to each other, due to the interference of the impurities, the superconductivity coherence peaks does not change a lot compared with the LDOS away from the two impurities; when the two impurities are located three or more sites away, the LDOS shows a case like the single impurity. Whereas, when the two impurities are located one or two sites away, we found the superconductivity coherence peaks are more strongly suppressed and the zero-energy peak have split into two peaks, which is qualitatively agreement with the experimental results.

Acknowledgements The authors would like to thank X. Yan and Dr. B. Liu for helpful discussions. This work was supported by the National Natural Science Foundation of China (Grant No. 10774082).

References

1. A. V. Balatsky and D. J. Scalapino, Phys. Rev. Lett., 1996, 77: 1841
2. A. V. Balatsky, I. Vekhter, and J. X. Zhu, Rev. Mod. Phys., 2006, 78: 373
3. P. W. Anderson, Science, 1987, 235: 1196
4. F. C. Zhang and T. M. Rice, Phys. Rev. B, 1988, 37: 3759
5. F. C. Zhang, Phys. Rev. Lett., 2003, 90: 207002
6. M. E. Flatte and J. M. Byers, Phys. Rev. Lett., 1997, 78: 3761
7. M. E. Flatte, Phys. Rev. B, 2000, 61: 14920
8. F. Yuan, Q. Yuan, and C. S. Ting, Phys. Rev. B, 2005, 71: 104505
9. J. X. Zhu and C. S. Ting, Phys. Rev. B, 2001, 64: 060501
10. J. X. Zhu, C. S. Ting, and A. V. Balatsky, Phys. Rev. B, 2002, 66: 064509
11. B. Liu and Y. Liang, Phys. Rev. B, 2008, 77: 245121
12. B. Liu, Phys. Rev. B, 2009, 79: 172501
13. Y. Chen and C. S. Ting, Phys. Rev. Lett., 2004, 92: 077203
14. A. Yazdani, C. M. Howald, C. P. Lutz, A. Kapitulnik, and D. M. Eigler, Phys. Rev. Lett., 1999, 83: 176
15. S. H. Pan, E. W. Hudson, K. M. Lang, H. Eisaki, S. Uchida, and J. C. Davis, Nature (London), 2000, 403: 746
16. E. W. Hudson, K. M. Lang, V. Madhavan, S. H. Pan, H. Eisaki, S. Uchida, and J. C. Davis, Nature (London), 2001, 411: 920
17. D. J. Derro, E. W. Hudson, K. M. Lang, S. H. Pan, J. C. Davis, J. T. Markert and A. L. de Lozanne, Phys. Rev. Lett., 2002, 88: 097002
18. D. K. Morr and N. A. Stavropoulos, Phys. Rev. B, 2002, 66: 140508
19. D. K. Morr, Phys. Rev. Lett., 2004, 93: 089902
20. D. K. Morr and J. Yoon, Phys. Rev. B, 2006, 73: 224511
21. A. Paramekanti, M. Randeria, and N. Trivedi, Phys. Rev. Lett., 2001, 87: 217002
22. F. Yang and T. Li, Phys. Rev. B, 2011, 83: 064524
23. W. S. Wang, X. M. He, D. Wang, Q. H. Wang, Z. D. Wang, and F. C. Zhang, Phys. Rev. B, 2010, 82: 125105
24. C. Chen, Y. Chen, Z. D. Wang, and C. S. Ting, Phys. Rev. B, 2010, 82: 174502